NUMERICAL STUDY OF HEAT AND MASS TRANSFER DURING EVAPORATION OF A THIN LIQUID FILM

by

M'hand OUBELLA[a], M'barek FEDDAOUI[b]*, and Rachid MIR[a]

[a] Laboratory for Mechanics, Energy and Environment
[b] Engineering Laboratory of Energy, Materials and Systems
National School for Applied Sciences, University Ibn Zohr, Agadir, Morocco

Original scientific paper
DOI: 10.2298/ TSCI130128145O

A numerical study of mixed convection heat and mass transfer with film evaporation in a vertical channel is developed. The emphasis is focused on the effects of vaporization of three different liquid films having widely different properties, along the isothermal and wetted walls on the heat and mass transfer rates in the channel. The induced laminar downward flow is a mixture of blowing dry air and vapour of water, methanol or acetone, assumed as ideal gases. A 2-D steady-state and elliptical flow model, connected with variable thermo-physical properties, is used and the phase change problem is based on thin liquid film assumptions. The governing equations of the model are solved by a finite volume method and the velocity-pressure fields are linked by SIMPLE algorithm. The numerical results, including the velocity, temperature, and concentration profiles, as well as axial variations of Nusselt numbers, Sherwood number, and dimensionless film evaporation rate are presented for two values of inlet temperature and Reynolds number. It was found that lower the inlet temperature and Reynolds number, the higher the induced flows cooling with respect of most volatile film. The better mass transfer rates related with film evaporation are found for a system with low mass diffusion coefficient.

Key words: *film evaporation, mixed convection, heat and mass transfer, vertical channel*

Introduction

Laminar mixed convection in vertical open channel flows with simultaneous heat and mass transfer between a flowing gas and a liquid wetting the walls have received considerable attention because they are important in many processes occurring in nature and engineering applications such as human transpiration, cooling of electronic equipment, refrigeration, air conditioning, desalination and many others.

Many studies were conducted which deal with different geometric configurations and various thermal and solutal boundary conditions. Lin *et al*. [1] examined the combined buoyancy effects of thermal and mass diffusion on laminar forced convection heat transfer in a vertical tube. They showed that heat transfer in the flow is dominated by the transport of latent heat owing to the evaporation of the thin liquid film and that the ratio of the latent heat flux to the sensible heat flux has a minimum for a fixed wall temperature. Evaporative cooling of a liquid film through interfacial heat and mass transfer in vertical ducts was investigated by Yan *et al*. [2], Yan and Lin [3], Yan [4], Feddaoui *et al.* [5, 6], and Feddaoui and Mir [7]. A liquid film

* Corresponding author; e-mail: m.feddaoui@uiz.ac.ma

streams along the plates with a temperature, which is higher than that of the downward airflow at the entrance. Their results showed that the influence of the evaporative latent heat transfer on the cooling of the liquid film depends largely on the inlet liquid film temperature and the inlet liquid mass flow rate. Huang *et al.* [8], and Jang and Yan [9] examined in detail the effects of the relative humidity of the moist air, wetted wall temperature, Reynolds number and aspect ratio of a vertical or an inclined rectangular duct with film evaporation along a porous wall, and with mixed convection in the entrance region. In their major results they confirmed the assumption of zero film thickness.

Hammou *et al.* [10] studied numerically the effects of the inlet conditions on a downward laminar flow of humid air in a vertical channel with isothermal wetted walls. Cases of film evaporation and vapour condensation were considered. The effect of thermal and solutal buoyancy forces on flow characteristics is significant. Azizi *et al.* [11] reconsidered the problem for both upward and downward mixed convection. According to the flow direction, the results show that in the case of relatively high temperature differences between ambient and isothermal wall flow reversal occurred for upward flows. Recently, Kassim *et al.* [12] investigated the effect of inlet air humidity in a humidifier. Their results show that the performances of the humidifier are seriously affected when increasing the air humidity at the channel entrance as it induces condensation of the water vapour on the walls.

The mentioned literature survey shows that the elliptic formulation has been systematically applied with the Boussinesq approximation and constant thermo-physical properties of humid air which are evaluated by the one-third rule as in [1]. This assumption was investigated by Laaroussi *et al.* [13] for simultaneous heat and mass transfer on laminar mixed convection in a vertical parallel-plate channel with film evaporation by considering two systems: air-water and air-hexane. They compared the Boussinesq and variable-density models at relatively high temperatures.

In the most of mentioned papers, the problem was studied for the water film evaporation with the assumptions of constant properties and Boussinesq approximation. Whereas, other liquids plays an important role in practical applications with large variations in thermophysical properties. This scope motivates the present study. The main objective of this work is to examine the effects of the evaporation of three pure thin liquid films (water, methanol, and acetone), selected for their large difference in properties, upon the heat and mass transfer rates in a vertical channel by analyzing the effect of the Reynolds number and inlet temperature of dry air on the film evaporation process.

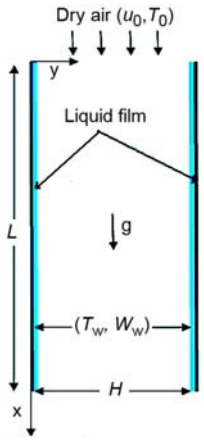

Figure 1. Schematic diagram of the channel and co-ordinate system

Problem description

Physical model and assumption

The physical model concerned in this study is a dry air flowing downward inside a vertical parallel plate channel of height L and a width H with co-ordinate systems as shown in fig. 1. The fluid, with constant properties corresponding to inlet temperature T_0, enters the vertical channel with uniform velocity u_0. The vertical plates of the channel are wetted by a thin liquid film of water, methanol or acetone and maintained at a constant temperature T_w.

For the mathematical formulation of the problem, the following simplifying assumptions are taking into consideration:

– the flow is laminar, steady and 2-D,
– the binary mixtures of water, methanol or acetone vapour and dry air, is supposed to be an ideal mixture of perfect gas,
– the effect of the superficial tension is neglected. The gas-liquid interface is in thermodynamic equilibrium, and
– radiation heat transfer, viscous dissipations and other secondary effects are negligible.

Governing equations

With the above assumptions, the steady mixed convection heat and mass transfer in vertical channel can be described by the following dimensionless governing equations.

$$\frac{\partial}{\partial x}(\rho u)+\frac{\partial}{\partial y}(\rho v)=0 \tag{1}$$

$$\rho u\frac{\partial u}{\partial x}+\rho v\frac{\partial u}{\partial y}=-\frac{\partial p}{\partial x}+\frac{\partial}{\partial x}\left(\mu\frac{\partial u}{\partial x}\right)+\frac{\partial}{\partial y}\left(\mu\frac{\partial u}{\partial y}\right)+\rho g \tag{2}$$

$$\rho u\frac{\partial v}{\partial x}+\rho v\frac{\partial v}{\partial y}=-\frac{\partial p}{\partial y}+\frac{\partial}{\partial x}\left(\mu\frac{\partial v}{\partial x}\right)+\frac{\partial}{\partial y}\left(\mu\frac{\partial v}{\partial y}\right) \tag{3}$$

$$\rho C_p u\frac{\partial T}{\partial x}+\rho C_p v\frac{\partial T}{\partial y}=\frac{\partial}{\partial x}\left(k\frac{\partial T}{\partial x}\right)+\frac{\partial}{\partial y}\left(k\frac{\partial T}{\partial y}\right) \tag{4}$$

$$\rho u\frac{\partial W}{\partial x}+\rho v\frac{\partial W}{\partial y}=\frac{\partial}{\partial x}\left(\rho D\frac{\partial W}{\partial x}\right)+\frac{\partial}{\partial y}\left(\rho D\frac{\partial W}{\partial y}\right) \tag{5}$$

Boundary conditions

– At the channel inlet ($x=0,\ 0<y<H$): $u=u_0,\ T=T_0,$ and $v=W=0,$ (6)

– At the walls ($y=0$ and $y=H$, $0<x<L$): $u=0,\ v=\pm v_e,\ T=T_{\mathrm{w}},$ and $W=W_{\mathrm{w}}.$ (7)

Here the transverse velocity at the interface is given:

$$v_e=-\frac{D}{1-W_{\mathrm{w}}}\left.\frac{\partial W}{\partial y}\right|_{y=0} \tag{8}$$

Heat and mass transfer parameters

Energy transport between the wetted walls and the air in the channel in the presence of mass transfer depends firstly on the fluid temperature gradient at the wetted walls, resulting in a sensible heat transfer and secondly on the rate of mass transfer, resulting in a latent heat transfer.

The local Nusselt number along the wall is defined:

$$\mathrm{Nu}_t=\frac{hd_h}{k}=\frac{q_t d_{\mathrm{h}}}{k\left(T_{\mathrm{w}}-T_{\mathrm{m}}\right)}=\mathrm{Nu}_{\mathrm{s}}+\mathrm{Nu}_{\mathrm{l}} \tag{9}$$

where h denote the local heat transfer coefficient, Nu_{s} and Nu_{l} are the local Nusselt numbers for sensible and latent heat transfer, respectively, and evaluated:

$$\mathrm{Nu_s} = \frac{-2\,H}{T_\mathrm{w} - T_\mathrm{m}} \left(\frac{\partial T}{\partial y} \right)_{y=0}, \qquad \mathrm{Nu_l} = \frac{-2\,H}{1 - W_\mathrm{w}} \frac{\rho D h_{fg}}{k\,(T_\mathrm{w} - T_\mathrm{m})} \left(\frac{\partial W}{\partial y} \right)_{y=0} \tag{10}$$

In a similar manner, the local Sherwood number on the wetted wall is give:

$$\mathrm{Sh} = \frac{h_\mathrm{m} d_h}{D} = \frac{-2H}{(1 - W_\mathrm{w})(W_\mathrm{w} - W_\mathrm{m})} \left(\frac{\partial W}{\partial y} \right)_{y=0} \tag{11}$$

In the present study, the thermo-physical properties of the gas mixtures are taken to be variable depending on temperature and concentration, they are calculated from the pure component data [14] by means of mixing rules [15] applicable to any multi-component mixtures.

Numerical method

The system of coupled, non-linear, elliptic partial differential eqs. (1)-(5), subject to their boundary conditions, has been solved numerically by using finite volume method. The velocity and pressure fields are linked by the semi-implicit method for linked equations (SIMPLE) algorithm proposed by Patankar, [16]. In order to get a mathematically well posed SIMPLE algorithm, overall continuity must be satisfied at outlet boundary, when computing the velocity field, and the outlet plane velocities with the continuity correction are given by [17]:

$$u_{NI,J} = u_{NI-1,J} \frac{\rho_0 u_0 H + 2\int_0^L \rho v_e \mathrm{d}x}{\int_0^H \rho u \mathrm{d}y} \tag{12}$$

The resulting set of discretization equations can be cast into a tri-diagonal matrix equation and solved iteratively using the TDMA algorithm. The criterion of convergence of the numerical solution is based on the absolute normalized residuals of the equations that were summed for all cells in the computational domain. Convergence was considered as being achieved when the largest residual of all variables falls below 10^{-6} at all grid points.

Grid independence

The physical domain was discretized into a structured grid, using the algebraic method for grid generation. A non-uniformed grid system was used, with greater node density near the inlet and the walls where the gradients are expected to be more significant. The grid refinement tests were carried out to ensure the independence of the calculations on several grid sizes. Table 1 presents the results of the local sensible Nusselt and Sherwood numbers and friction coefficient for each of these grid systems. It is clear that changes in $\mathrm{Nu_s}$, Sh, and f_Re with respect to the grid refinement are less than 1.5%. Therefore, to optimize CPU resources with an acceptable level of accuracy, all parametric runs were made with the 200 × 50 grid.

Code validation

The developed code based on the mathematical model above is validated in three ways by reproducing solutions for some results in the literature.

Laminar mixed convection with thermal diffusion.

The code is validated with two different cases. First, a combined forced and laminar mixed convection problem using the Boussinesq approximation is chosen, a vertical parallel

Table 1. Comparison of local sensible Nusselt and Sherwood numbers and friction coefficient for various grids, in case of air-water system with Re = 300, γ = 1/100, T_w = 20 °C, and T_0 = 30 °C

x [m]	0.1			1.0			1.5			1.96		
Grid (x, y)	Nu_s	Sh	f_{Re}	Nu_s	Sh	f_{Re}	Nu_s	Sh	f_{Re}	Nu_s	Sh	f_{Re}
100×30	8.791	8.707	47.90	7.546	7.548	24.57	7.514	7.514	23.59	7.508	7.508	23.34
150×40	8.783	8.703	48.40	7.560	7.561	24.56	7.528	7.528	23.64	7.523	7.523	23.45
200×50	8.732	8.666	48.27	7.564	7.566	24.55	7.535	7.535	23.66	7.530	7.529	23.43
250×60	8.777	8.701	48.80	7.568	7.569	24.56	7.538	7.539	23.66	7.533	7.533	23.45
300×70	8.738	8.632	47.90	7.562	7.499	24.72	7.535	7.490	23.58	7.534	7.500	23.12

plate channel of aspect ratio γ = 1/50 with a constant and uniform temperature at the boundaries is selected T_0 = 10 °C and T_w = 60 °C. The working fluid is air, which enters at the bottom of the channel with uniform velocity profile, Re = 300, the Grashof number is varied ($4.71\cdot10^4 \leq Gr_T \leq 1.27\cdot10^6$) by varying the width of the channel (0.02 m $\leq H \leq$ 0.06 m). Results of the local Nusselt number along the non-dimensional axial length (x/d_h Pe) are compared with results of Desrayaud and Lauriat [18].

The second comparison is done for parabolic velocity profile, considering the same problem as in first case, for the specific case of $Gr_T = 1.59\cdot10^5$, H = 0.03 m. A good agreement is observed as shown from fig. 2(a). The results presented in fig. 2(b) shows good agreement between the present work and those in [18] for centerline and bulk temperatures profiles. The discrepancies are less than 2%.

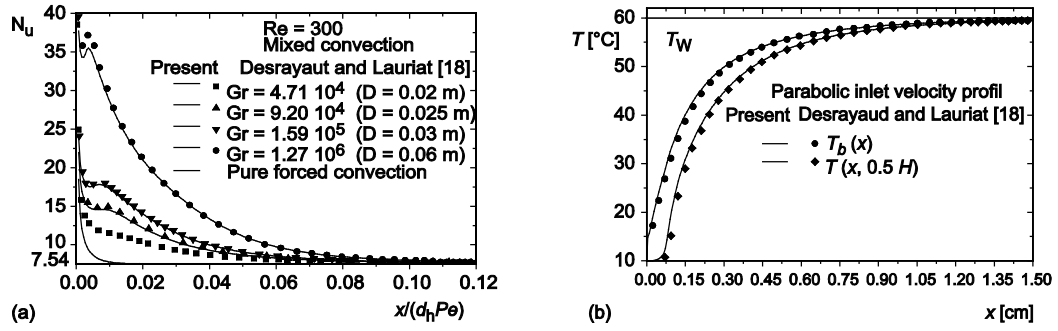

Figure 2. Validation of calculated (a) Nusselt number at the walls, (b) centerline and bulk temperature

Laminar mixed convection with solutal diffusion

The comparison is done for a vertical channel of aspect ratio γ = 1/100 with constant and equal temperature at the boundaries ($T_0 = T_w$ = 327.5 K), (Gr_T = 0). Dry air entered the channel with uniform downward velocity and Re = 300, the vertical parallel plates are wetted with water (W_w = 0.1 $kg_{vapour}kg^{-1}_{air}$). Figure 3 shows a comparison of velocity profiles calculated by Laaroussi *et al.* [13] and our results using the Boussinesq approximation, which are in excellent agreement, where the largest velocity difference is about 2.5%.

Laminar mixed convection with thermosolutal diffusion

A comparison with a published study by Hammou *et al.* [10] for small mass flow rates was also carried out. The working fluid is humid air, three values of the humidity and

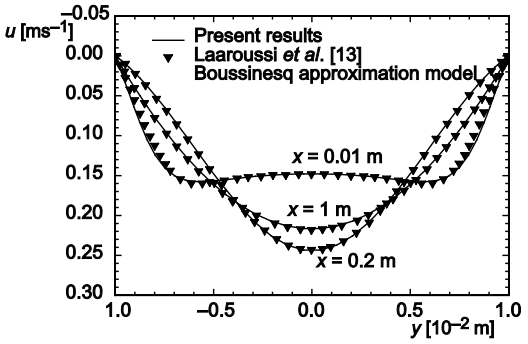

Figure 3. Comparison of vertical velocity profile for Re = 300, W_w = 0.1

Table 2. Values of parameters for cases of comparison

Case #	T_0 [°C]	ϕ_0 [%]	W_0 [gkg^{-1}]	Gr_T	Gr_M
1	40	10	4.56	–74576	7142
2	40	30	13.90	–74717	559
3	40	50	23.52	–74860	-6123
4	45	10	5.49	–89975	6042
5	30	10	2.62	–40077	8876

temperature at the inlet section were considered (tab. 2). In all cases, the wall temperature was T_w = 20 °C, (W_w = 14.5 gkg^{-1}) the channel aspect ratio was γ = 1/65, Pr = 0.7, Sc = 0.58, and Re = 300. Figures 4(a) and (b) show a comparison of transverse velocity profiles at the interface, and axial evolution of the average mass fraction, calculated by using the Boussinesq approximation; the present results are in excellent agreement with those reported in [10].

Through, these program tests and successful comparisons, we conclude that the model and the present numerical code are considered to be suitable for the present investigation.

Results and discussion

This study will examine the effects of the evaporation of three different thin liquid films, which exhibits different volatilities, on the heat and mass transfer rates. The induced flow is a mixture of the blowing dry air and vapour of the liquid film. Heat and mass transfer for the mixed convection depends on the dimensionless parameters Gr_T, Gr_M, Pr, and Sc which are interdependent for a given mixture, and cannot be arbitrarily assigned. Instead, the temperature of the dry air and Reynolds number at the inlet section are introduced as the independent variables for water, methanol and acetone thin film evaporation. The numerical simulations assume the following conditions: T_w = 20 °C and γ = 1/100. The inlet Reynolds number was assigned 300 and 900, and two values of the inlet temperature T_0 = 30 °C and 60 °C. The thermo-physical properties and operating conditions used for the simulation and other relevant parameters are presented in tabs. 3 and 4, respectively.

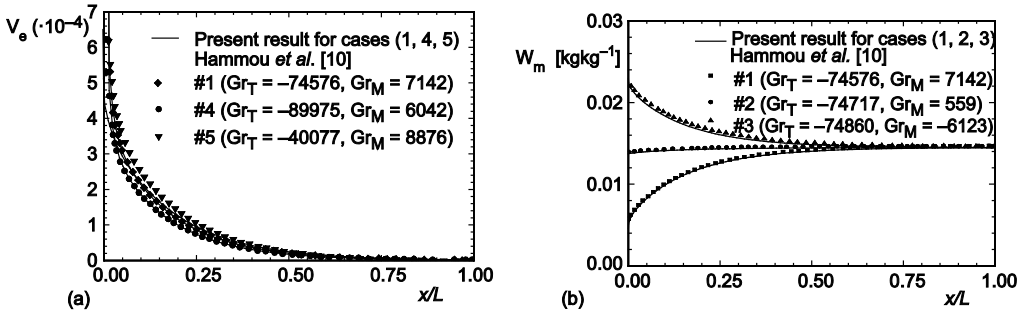

Figure 4. Validation of calculated (a) transverse velocity at the interface, (b) axial evolution of the average mass fraction

The thin liquid films properties shown in tab. 3 indicate the notable differences between the three fluids, particularly, acetone has the lowest latent heat of vaporization, then

Table 3. Thermo-physical properties of the gas mixtures given for an interfacial film temperature T = 298 K

Liquid film	M [gmol^{-1}]	T_b [°C]	p_{sat} [kPa]	ρ_m [kgm^{-3}]	μ_m [Nm^{-1}s^{-1}]	h_{fa} [kJkg^{-1}]	D [m^{2}s^{-2}]
Water	18.015	100	2.137	1.196	$1.792\cdot10^{-5}$	2432.7	$2.518\cdot10^{-5}$
Methanol	32.042	65	12.80	1.221	$1.768\cdot10^{-5}$	1196	$1.573\cdot10^{-5}$
Acetone	58.08	56.5	24.50	1.480	$1.330\cdot10^{-5}$	561.2	$1.061\cdot10^{-5}$

Table 4. Values of parameters for cases under study

System	T_w [°C]	W_w [gkg^{-1}]	β_M	T_0 [°C]	Gr_T (10^4)	Gr_M (10^4)	N	Pr	Sc
Air-water	20	14.44	0.607	30	–08.11	02.16	–0.266	0.708	0.597
	20	14.44	0.607	60	–21.13	01.54	–0.073	0.703	0.593
Air-methanol	20	139.00	-0.097	30	–08.36	–03.41	0.408	0.709	1.132
	20	139.00	-0.097	60	–23.92	–02.68	0.112	0.707	1.277
Air-acetone	20	384.14	-0.552	30	–08.36	–53.76	6.431	0.709	1.678
	20	384.14	-0.552	60	–23.92	–42.26	1.767	0.707	1.893

methanol is higher, and water has the highest latent heat of vaporization. On the other hand, acetone is the most volatile (lower boiling temperature, T_b = 56.5 °C) and heavier among all the two liquid films.

The magnitudes of the buoyancy forces for each system can be parameterized through thermal and solutal Grashof numbers Gr_T and Gr_M. Since the temperature of wall is less than the inlet temperature ($T_w < T_0$), it is noticed for all cases listed in tab. 4, the thermal Grashof number are negative, thus the corresponding buoyancy acts in the direction of the air flow. The solutal Grashof number may be positive or negative, it's sign depending on the solutal coefficient of volumetric expansion. The relative importance of thermal and solutal buoyancy forces is denoted by the buoyancy ratio N, and is defined as the ratio between the solutal and thermal buoyancy forces:

$$N = \frac{Gr_M}{Gr_T} = \frac{\beta_M (W_w - W_0)}{\beta_T (T_w - T_0)} \tag{13}$$

where β_M is evaluated at the reference mass fraction W_r calculated by using the one-third rule [13].

Due to weak buoyancy ratio ($-1 < N < 0$), the air-water system is characterized by thermal-dominated opposing flow. For the air-methanol system, the small value of the ratio ($0 < N < 1$) indicating that the induced flow is influenced by thermal buoyancy which act in the flow direction. For the case of air-acetone system the buoyancy ratio is larger than unity, thus the solutal buoyancy forces are prevalent and aiding flow.

Velocity, concentration, and temperature profiles

Attention was paid to the comparison of velocity, temperature and concentration profiles for the three flows systems, because of their usefulness in clarification of evaporation

phenomenon between the wetted parallel plates. The Reynolds number is fixed at Re = 300 and the inlet temperature at T_0 = 30 °C.

Axial velocity profiles

Figure 5 shows a comparison of the development of the axial velocity profiles for the three systems at different axial location in the channel. The difference in the shape of the axial velocity profiles between these three systems is very significant, close to the channel entrance (x = 0.1 m) the velocity of the induced flow for the air-water system is relatively uniform, because of the weak effect of buoyancy forces, as the flow moves downstream, the parabolic velocity profile is developed with the maximum velocity in the core region. As can be seen at the same position for the air-methanol system, the magnitude of upward velocities is less important at the channel center, comparing to the air-acetone system ones, near the walls, we noticed slow flow acceleration, due to the mass diffusion. Since the Schmidt number is great than unity, the solutal forces effects are greater than viscous ones in the solutal boundary layers comparing to the air-water system (in which viscous forces are prevalent). As the flow goes downstream, the velocity profiles develop gradually to distort ones with the maximum velocity at the channel center in comparison with air-acetone flow. This last flow system presents significantly distorted axial velocity profile, near the wetted walls the velocity presents its maximum value (u = 0.25 m/s) larger than the two first systems, and in order to maintain the overall mass balance, the induced flow in the core region is decelerated and the velocity takes negative value, indicating reversed flow. This is explained by the larger Schmidt number value (Sc = 1.678), the prevalence of solutal buoyancy forces which overcome the viscous ones in the boundary layers and the large mass evaporation rates (W_w = 384.14 g/kg) in the in-

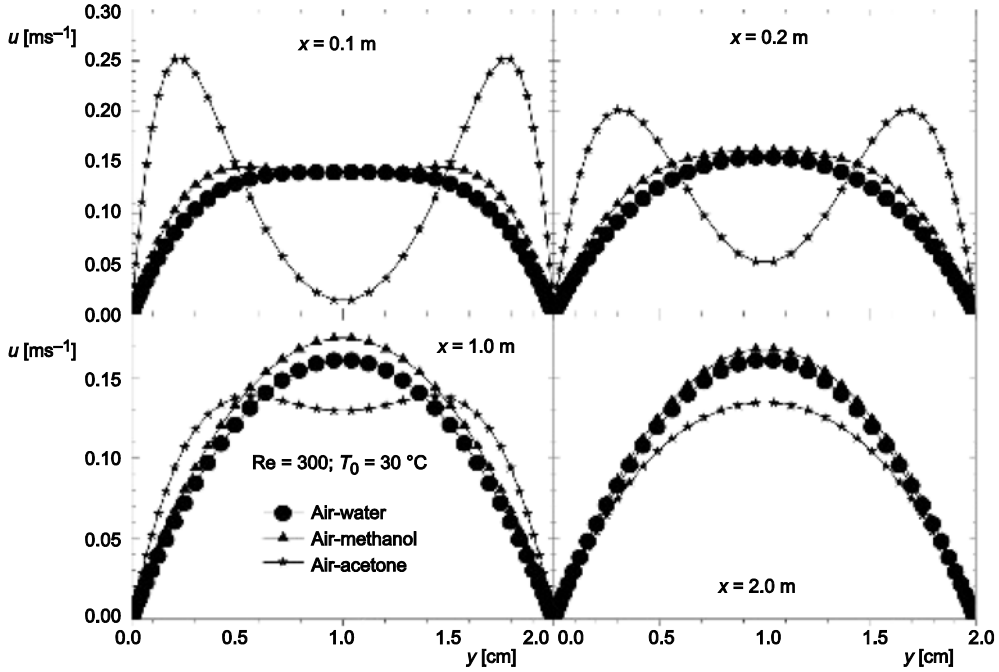

Figure 5. Axial velocity profiles at different axial location

let section. In other words, the flow acceleration increases near the walls with the increase of molecular weight and the large changes in the mixture density at the channel entrance. From the inlet to the outlet sections of the channel, the two symmetrically velocity maximums are gradually recovered and finally disappearing, the maximum velocity reached at the outlet is less than the two others systems.

Axial concentration and temperature profiles

The developments of mass-fraction and temperature profiles are shown in figs. 6 and 7, by comparing the concentration curves of the three flows systems, it is found that they don't develop in a similar manner, this is explained by the fact that each liquid film has its own volatility and then evaporates at different rates which results in a different mass fraction vapour in the induced flow. Also to be seen in fig. 6 is that the concentration boundary layer thickness becomes shorter as the thin liquid film is more volatile, in other words, it is generally smaller as the Schmidt number increase and this one specifies the molecular diffusion of different liquid film. Larger value of Schmitt number corresponds to smaller molecular diffusion and hence for large Schmidt number (see tabs. 3 and 4). The comparison between concentration and temperature profiles from figs. 6 and 7 indicates that these curves develop in a similar fashion. Closer inspection, however, reveals that temperature profiles develops slightly more rapidly than those of concentrations except for the profiles of air-water flow, which exhibits the opposite behaviour. For this last case the mass fraction boundary layer develops more rapidly than the thermal one, this is because that the Pr = 0.708 is greater than

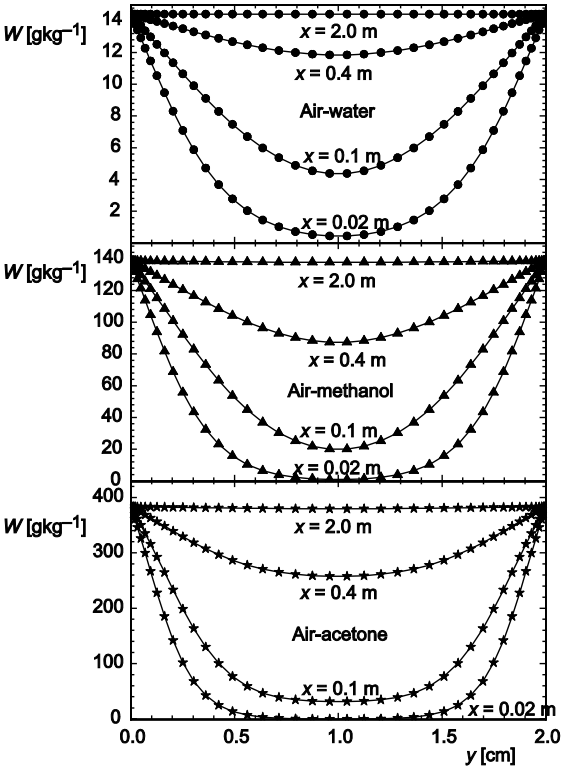

Figure 6. Concentration profiles

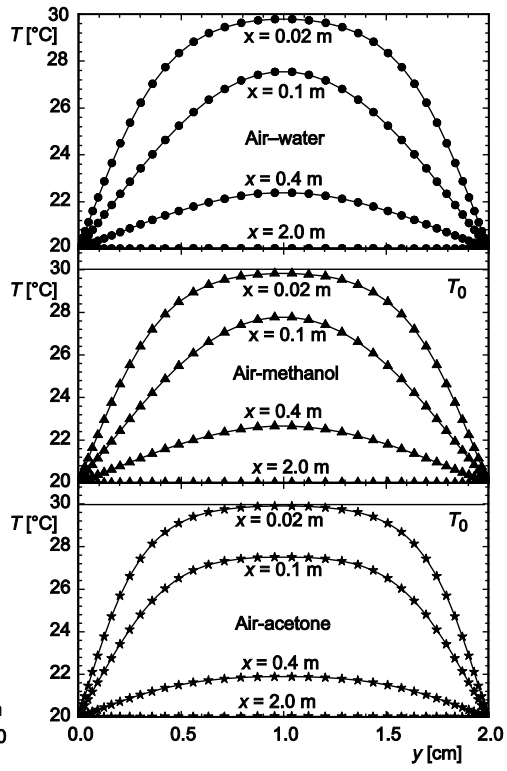

Figure 7. Temperature profiles

Sc = 0.597, which exerts the reverse influence since it corresponds to higher molecular diffusivity. For the air-methanol and air-acetone systems thermal boundary layers are thicker than those of concentration, this is due to the fact that the Schmidt number is greater than Prandtl number. Acetone liquid film vaporizes more rapidly than methanol and water films which reduce monotonically the average temperatures of the induced flows from the inlet temperature T_0 = 30 °C to attain T_w = 20 °C at the channel exit. This is explained by the fact that acetone film has the lowest latent heat of vaporization and high volatility comparing to methanol and water ones (see tab. 4).

Effect of evaporation conditions

To investigate the effect of evaporation conditions in the channel, two simulations with different Reynolds number were performed, Re = 300 and Re = 900, respectively, while the inlet temperature is kept constant at T_0 = 30 °C. Shown in figs. 8(a) and (b) are the distribution of the local Nusselt numbers (Nu_s and Nu_l), for the three flow systems, along the wetted wall whose temperature is fixed at T_w = 20 °C. Before examining these results, it would be interesting to discuss their common behaviour for the two inlets Reynolds numbers. According to the results in figs. 8(a) and (b) the differences in latent Nusselt numbers plots is considerably higher, also comparing the ordinate scales of the air-methanol and air-acetone systems points out that the magnitude of Nu_l is relatively very larger than that of sensible Nusselt numbers (Nu_s) over the entire channel length. Therefore the heat transfer due to the transport of latent heat is predominant than that due to the transport of the sensible heat in the wall. Also, by comparing the two

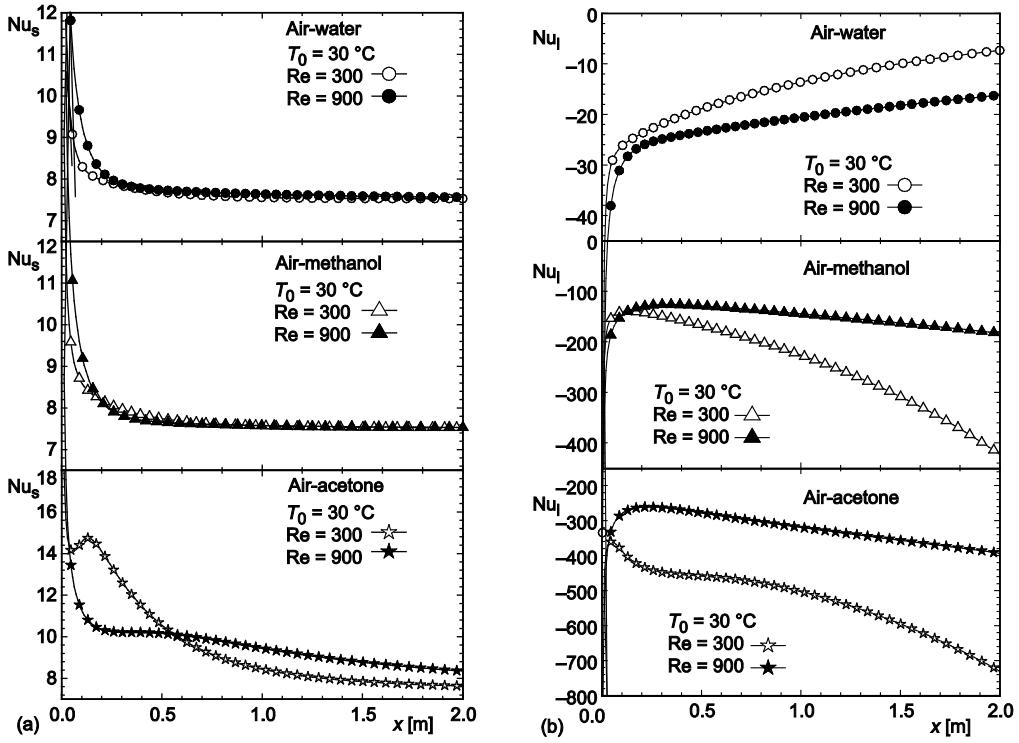

Figure 8. Effect of inlet Reynolds number on the axial distributions of (a) sensible Nusselt number, (b) latent Nusselt number, for the three systems evaporation

last flow systems to the air-water flow under the same dynamic and thermal conditions, the heat exchange during the evaporation of the thin film liquid of acetone and methanol is much effective than that with water film evaporation. Additionally, referring to the expression of latent Nusselt number eq. (10), Nu_l profiles are negative, because the wall temperature is less than the average one ($T_w < T_m$), on the other hand the Nu_s is positive as seen in eq. (10), thus the direction of latent heat exchange is opposed to that of sensible heat exchange as reported by [19].

It is seen from figs. 8(a) and (b) that increasing the Reynolds number (inlet dry air velocity) the following features are exhibited.

Regarding Nu_s-plots, at the channel entrance the sensible Nusselt number increases slightly for the two cases of air-water and air-methanol systems, as the induced flow moves downstream Nu_s decreases monotonically towards the same asymptotic value at the channel outlet which is equal to the analytical value for fully developed flow in forced convection ($Nu_s = 7.54$), this tendency has also been reported by many authors for the case of air-water flow [1,10]. This behaviour is absent in the case of air-acetone flow, for which Nu_s exhibits local minimum ($x = 0.05$ m, $Nu_s = 14.1$) and maximum ($x = 0.13$ m, $Nu_s = 14.74$) that corresponds to the flow reversal at the channel entrance for Re = 300, then Nu_s decreases monotonically towards the channel exit. When Re = 900, one can sees the disappearance of extremums and in the first quarter of the channel the Nu_s values are less than those with Re = 300. At position $x = 0.55$ m and greater the Nu_s profile overcomes the ones with Re = 300.

Regarding Nu_l-plots, in fig. 8(b), the Nu_l decreases at the downstream with the decease of Re for the two systems of air-methanol and air-acetone, while increases with the decrease of Reynolds number for the case of air-water system. Also it should be noted that for this last system the sum of Nu_s and Nu_l numbers, which is the total heat transfer changes the sign to be positive at location $x = 1.5$ m, this is explained by the fact that Nu_s is greater than Nu_l after this location, therefore, the energy is transported from the wetted wall to gas stream through condensation. By comparing curves for sensible and latent Nusselt number of the three flow systems, it was found that under the same thermal and hydro-dynamical conditions, the mixed heat transfer associated with acetone film evaporation is much effective than that with methanol and water films evaporation, respectively.

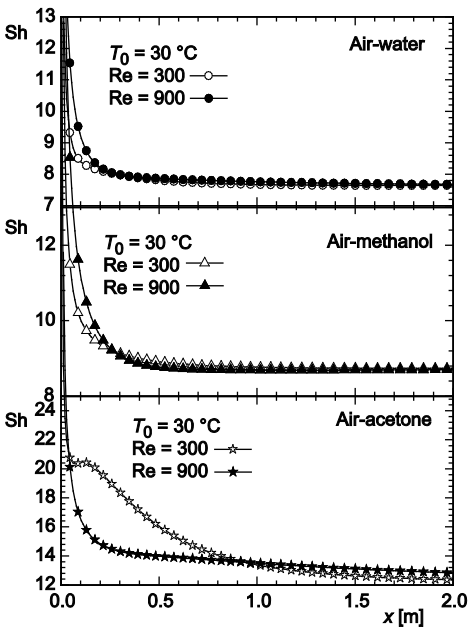

Figure 9. Effect of inlet Reynolds number on the axial distributions of local Sherwood numbers for the three systems evaporation

To characterize the masse transfer, the variations of local Sherwood number along the wetted wall for Re = 300 and Re = 900 are depicted in fig. 9. It is clearly seen that results are similar in trend to those of the sensible Nusselt number. By comparing Sherwood number and Nu_s curves of the three flow systems, it is found in figs. 8(a) and 9 a similar behaviour is noted for the local Sherwood number and Nu_s. This is because the Prandtl number and Sherwood number are the same order of magnitude (tab. 4). For the two other flow systems (air-methanol, air-acetone), it is clear that in figs. 8 and 9 the

magnitude of Sherwood number is relatively greater than that of Nu_s number. This is owing to the fact that the Schmidt numbers are greater than Prandtl numbers as shown in tab. 4. Air-acetone flow shows the highest local Sherwood number (among all the two flows systems) with variation of Reynolds number, owing to the large concentration gradient at the wall and the lower mass diffusion coefficient.

Effect of evaporation temperature

The effect of evaporation temperature is investigated by comparing two different inlet air temperatures at 30 °C and 60 °C while the Reynolds number is fixed at 300. The results shown in figs. 10(a) and (b) follow the same trend seen earlier in the previous section. As expected, increasing the air temperature leads to increasing the three kinds of Nusselt numbers with associated changes in thermo-physical properties. However, the heat transfer rate of acetone film is lower than the other liquid films because of its very low latent heat of vaporization. The variations of Nu_s are similar to those discussed previously for air-water and air-methanol systems, however, near the entrance large Nu_s is noted for a higher inlet temperature. Careful scrutiny on figures of air-water system for the case of T_0 = 60 °C discloses that the magnitude of Nu_s is relatively larger than that of Nu_l, therefore the total Nusselt number heat transfer is positive everywhere, indicating that the heat is transferred from the channel wall to the air stream. The Nu_s-plots of air-acetone flow exhibits slight increase at the entrance and merge at the exit with the increase of T_0.

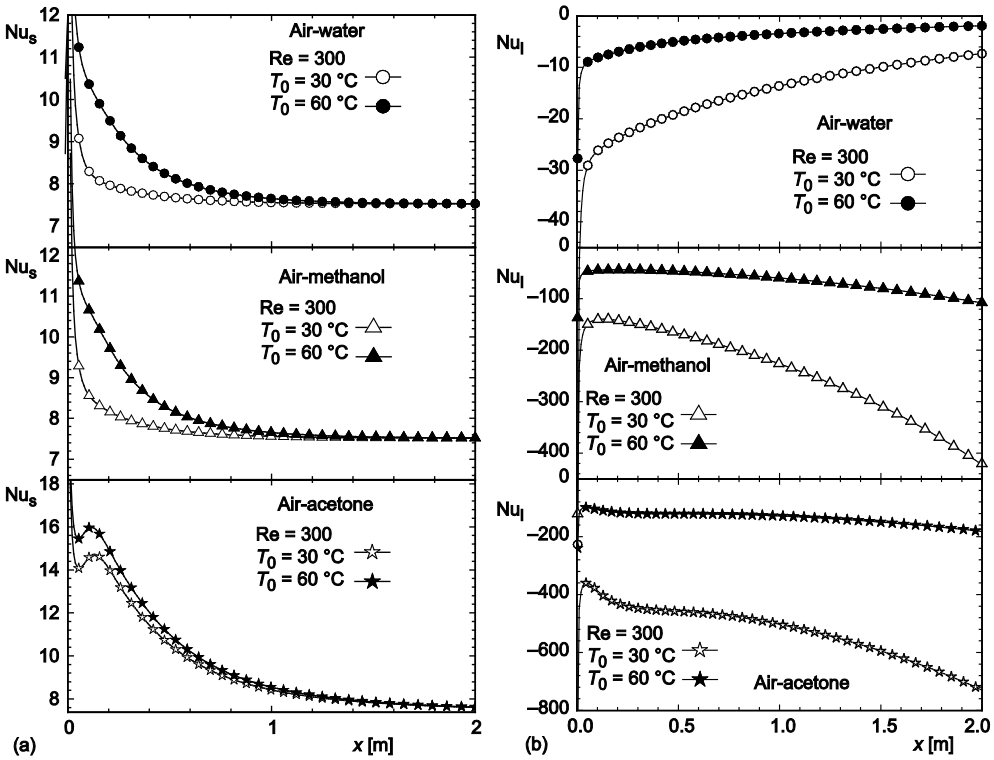

Figure 10. Effect of inlet temperature on the axial distributions of local Nusselt numbers of (a) sensible Nusselt number and (b) latent Nusselt number, for the three systems evaporation

By analyzing Nu_l-curves, it is found that near the entrance the Nu_l increases as T_0 increases, the difference between the two Nu_l-plots corresponding to T_0 = 60 °C and T_0 = 30 °C decreases slightly towards the channel exit for the air-water system, while this difference increases for the two others systems. Thus the cooling of the induced flows is enhanced with the decreasing of T_0, because acetone film has large latent Nusselt number, the stream gas cool significantly during vaporisation than methanol and water films, respectively, as previously shown in fig. 7.

Effect of temperature and Reynolds number on the net mass flow rate

As mentioned, interfacial heat and mass transfer in the wetted wall system is dominated by film vaporisation. Therefore, the amount of vapour added to the gas stream due to film vaporisation is important for a more volatile component in improving our understanding of the heat and mass transfer rates. To quantify the film evaporation a nondimensional accumulated mass evaporation rate, *Mr* is introduced:

$$Mr = \frac{\int_0^L \rho v_e \mathrm{d}x}{\rho_0 u_0 H} \tag{14}$$

The effect of Reynolds number and inlet temperature on the distributions of dimensionless accumulated mass evaporation rate are illustrated in fig. 11. The larger *Mr* is found for a system with smaller Reynolds number and higher T_0, however the effect of T_0 is relatively insignificant, the more volatile the liquid film is and the less important the heating is. By comparing *Mr*-curves, the larger thin film evaporation is observed for the air-acetone flow followed by air-methanol flow and in the last the air-water flow. The largest *Mr* with effects of system Reynolds number and T_0 are: 28%, 7.8%, and 0.73%, respectively.

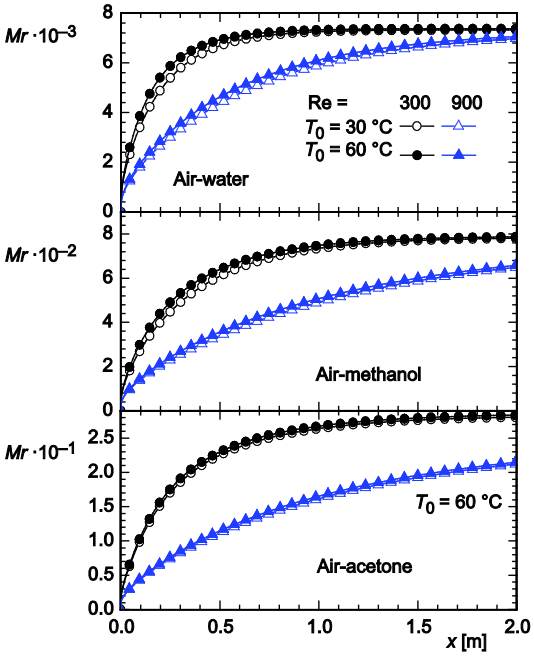

Figure 11. Effect of inlet temperature on the axial distributions of accumulated evaporation rate, for the three systems evaporation

Conclusion

This paper presents numerical simulation of the evaporation on laminar mixed convection in a vertical channel formed by two parallel plates, which are isothermal and wetted by a thin liquid film of water, methanol or acetone. The effects of inlet dry air temperature and Reynolds number on the heat and mass transfer rates were particularly investigated. The major results are briefly summarized as follows.

- Flow acceleration near the walls is larger for liquid films, which are more volatile and heavy.
- The influence of the latent Nusselt numbers on the cooling of induced flows by evaporation depend largely on the inlet temperature and Reynolds number. It was shown that the

lower is T_0 and Reynolds number, the higher the induced flows cooling. Air-acetone mixture cools more significantly during vaporization than air-methanol and air-water mixtures, respectively.

- Increasing of inlet temperature leads to large mass transfer rate for air-acetone system followed by air-methanol and at the last air-water system. Thus the better mass transfer rates related with film evaporation are found for a system with low mass diffusion coefficient. Furthermore, the lower boiling point is favourable for mass transfer.
- The dimensionless masse evaporating rate increases noticeably with decreasing Reynolds number and the use of more volatile thin liquid film, while increasing inlet temperature is insignificant.

Nomenclature

C_p – specific heat, [Jkg^{-1}K^{-1}]
D – mass diffusion coefficient, [m^{2}s^{-2}]
d_h – hydraulic diameter, [m]
f_{Re} – friction factor,
Gr_M – solutal Grashof number, $[= g\beta_M d_h^3(W_w - W_0)\nu^2]$, [–]
Gr_T – thermal Grashof number $[= g\beta_T d_h^3(T_w - T_0)\nu^2]$), [–]
h_{fg} – latent heat of vaporization, [Jkg^{-1}]
k – thermal conductivity, [Wm^{-1}K^{-1}]
p – mixture pressure, [Pa]
p_{sat} – saturation pressure, [Pa]
W – mass fraction, [–]
x, y – Cartesian co-ordinate, [m]

Greek symbols

α – thermal diffusivity, [m^{2}s^{-1}]
β_T – thermal coefficient of volumetric expansion, $(= 1/T_0)$, [K^{-1}]
β_M – solutal coefficient of volumetric expansion,
γ – aspect ratio, $(= H/L)$, [–]

Subscripts

0 – inlet condition
a – dry air
v – vapor
m – mixture
T – thermal
w – wall condition

References

[1] Lin, T. F., *et al*., Analysis of Combined Buoyancy Effects of Thermal and Mass Diffusion on Laminar Forced Convection Heat Transfer in a Vertical Tube, *ASME J. Heat Transfer, 110* (1988), 2, pp. 337-344
[2] Yan, W. M., *et al*., Evaporative Cooling of Liquid Film through Interfacial Heat and Mass Transfer in a Vertical Channel – I. Experimental Study, *Int. J. Heat Mass Transfer, 34* (1991), 4-5, pp. 1105-1111
[3] Yan, W. M., Lin, T. F., Evaporative Cooling of Liquid Film through Interfacial Heat and Mass Transfer in a Vertical Channel – II. Numerical Study, *Int. J. Heat Mass Transfer*, *34* (1991), 4-5, pp. 1113-1124
[4] Yan, W. M., Evaporative Cooling of Liquid Film in Turbulent Mixed Convection Channel Flows, *Int. J. Heat Mass Transfer*, 41 (1998), 23, pp. 3719-3729
[5] Feddaoui, M., *et al*., Numerical Study of the Evaporative Cooling of Liquid Film in Laminar Mixed Convection Tube Flows, *Int. J. Therm. Sci.*, *40* (2001), 11, pp. 1011-1019
[6] Feddaoui, M., *et al*., The Numerical Computation of the Evaporative Cooling of Falling Water Film in Turbulent Mixed Convection inside a Vertical Tube, *Int. Comm. Heat and Mass Transfer, 33* (2006), 7, pp. 917-927
[7] Feddaoui, M., Mir, A., Turbulent Mixed Convection Heat and Mass Exchanges in Evaporating Liquid Film along a Vertical Tube, *Int. J. Heat Exchangers*, *8* (2007), pp. 15-31
[8] Huang, C.-C., *et al*., Laminar Mixed Convection Heat and Mass Transfer in Vertical Rectangular Ducts with Film Evaporation and Condensation, *Int. J. Heat Mass Transfer*, *48* (2005), 9, pp. 1772-1784
[9] Jang, J.-H., Yan, W.-M., Thermal Protection with Liquid Film in Turbulent Mixed Convection Channel Flows, *Int. J. Heat Mass Transfer, 49* (2006), 19-20, pp. 3645-3654
[10] Hammou, Z. A., *et al*., Laminar Mixed Convection of Humid Air in a Vertical Channel with Evaporation or Condensation at the Wall, *Int. J. Therm. Sci., 43* (2004), 6, pp. 531-539
[11] Azizi, Y., *et al*., Buoyancy Effects on Upward and Downward Laminar Mixed Convection Heat and Mass Transfer in a Vertical Channel, *Int. J. Numer. Methods Heat Fluid Flow, 17* (2007), 3, pp. 333-353
[12] Kassim, M. A., *et al*., Effect of Air Humidity at the Entrance on Heat and Mass Transfers in Humidifier intended for a Desalination System, *Applied Thermal Engineering, 31* (2011), 11-12, pp. 1906-1914

[13] Laaroussi, N., *et al*., Effects of Variable Density for Film Evaporation on Laminar Mixed Convection in a Vertical Channel, *Int. J. Heat Mass Transfer, 52* (2008), 1-2, pp. 151-164
[14] Perry, D., *Perry's, Chemical Engineers' Handbook*, Mc Graw-Hill, New York, USA, 1999
[15] Reid, R. C., *et al*., *The Properties of Gas and Liquid*, Hemisphere, McGraw-Hill, New York, USA, 1977
[16] Patankar, S. V., *Numerical Heat Transfer and Fluid Flow*, Hemisphere, New York, USA, 1980
[17] Versteeg, H. K., Malalasekera, W., *An Introduction to Computational Fluid Dynamics: the Finite Volume Method*, Longman Scientific & Technical, London, 1995
[18] Desrayaud, G., Lauriat, G., Heat Flow Reversal of Laminar Convection in the Entry Region of Symmetrically Heated, Vertical Plate Channels, *Int. J. Therm. Sci.*, *48* (2009), 11, pp. 2036-2045
[19] Yan, W. M., Lin, T. F., Combined Heat and Mass Transfer in Laminar Forced Convection Channel Flows, *Int. Comm. Heat Mass Transfer, 15* (1988), 3, pp. 333-343

Paper submitted: January 28, 2013
Paper revised: November 3, 2013
Paper accepted: November 5, 2013